Strain transfer modeling of distributed optical fiber sensors under any arbitrary strain distribution: a general solution

Xavier Chapeleau

Optical Fiber Sensors (OFS) 2022 © Optica Publishing Group 2022

Strain transfer modeling of distributed optical fiber sensors under any arbitrary strain distribution: a general solution

Xavier Chapeleau
COSYS-SII, I4S Team (Inria), Université Gustave Eiffel, Allée des Ponts et Chaussées, 44344 Bouguenais, France
xavier.chapeleau@univ-eiffel.fr

Abstract: This paper is concerned with the strain transfer modeling of distributed optical fiber sensors. A general solution describing the strain transfer for any arbitrary strain distribution is introduced. Then, experimental results of validation are presented.

Introduction

To prevent damage during installation and monitoring in harsh environments, the optical fiber or cable used for distributed strain measurements [1, 2] are always surrounded by one or several stacks of coatings made of different materials. As consequence, a mechanical strain transfer occurs [3]. This means that a strain lag exists between the strain in the core of the optical and the one at outer of the optical fiber/cable that is sought to be measured. It is important to precise that the strain transfer occurs on small distance (typically few centimeters). As consequence, it affects only the strain profiles measured by high-resolution distributed strain sensing systems such as the one based on the measurement of the Rayleigh back-scattering by OFDR (Optical Frequency Domain Reflectomer). In the presence of high strain gradients such as those induced by the presence of a singularity (crack) or by a particular geometry or heterogeneous assembly of different materials, the strain transfer can lead to misinterpretation of the high-resolution strain distributed measurements. To correctly interpret them, it may therefore be necessary to better understand and modelize the strain transfer of optical fibers/cables.

The first part of the paper presents the governing equation of the strain transfer which is characterized by a coefficient called strain lag paramater. In the second part, a general solution for determining the strain in the core of the optical fiber under any arbitrary strain distribution is introduced. In the last part, experimental results of validation are presented.

1. Analytical modeling of strain transfer: governing equation

Depending on the structure to be monitored, two optical fiber installation configurations can be used. For concrete structures in construction, distributed optical cables can be embedded in concrete or glued in rebars before pouring. For steel structures or existing concrete structures, they are generally glued directly on surface with adhesives or introduced inside a surface groove filled with an adhesive. For these both installation configurations, embedded into host material and bonded on surface, strain in the host material is transferred into the core of the optical fiber (the sensing part) by shear stresses. Consequently, the geometry and the mechanical properties of the optical fiber's coatings play a major role in the strain transfer as well as the type of optical fiber installation configuration. For embedded optical fiber, it has been shown in [4] that interface stiffness of the interface between the embedded optical cable and the host material is also an important factor. For bonded optical fiber, the distance for a complete strain transfer from the host material to the core of the fiber sensor is longer for soft adhesives (such as silicone) than for stiff adhesive (such as epoxy) as shown in [5].

Several analytical modelings have been proposed to describe the strain transfer for both embedded and surface bonded optical fibers with different numbers of coatings [6, 7]. The most recent ones include also the adhesive layer and the imperfect bonding between the optical fiber and the host material [8, 9]. All these analytical modelings rely on the same basics of mechanics. They permit to derive a governing equation that links the strain in the core of the optical fiber sensor $\epsilon_f(x)$ to the strain in the host material $\epsilon_m(x)$ by a second-order differential equation as the following:

$$\frac{d^2\epsilon_f(x)}{dx^2} - \beta^2\epsilon_f(x) = -\beta^2\epsilon_m(x) \qquad (1)$$

where β is a constant parameter, called strain-lag parameter. Only the expression of this parameter is changing for the different modeling, either embedded or surface bonded optical fiber as mentioned in [10].

2. General solution for determining the strain profile $\epsilon_f(x)$ under any arbitrary strain profile $\epsilon_m(x)$

From Eq. 1, the strain in the optical fiber $\epsilon_f(x)$ can be determined analytically and numerically for any arbitrary strain distribution $\epsilon_m(x)$ existing along the optical fiber. Recently, a new set of boundaries conditions has been proposed [10] in order to better match the real cases.

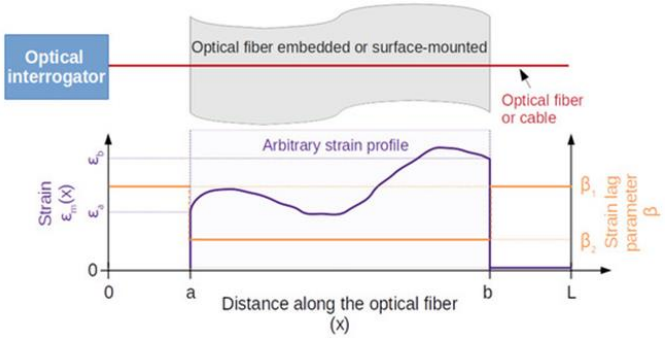

Fig. 1. Strain lag parameter along an optical fiber used to measure an arbitrary strain profile $\epsilon_m(x)$ (between the abscissas *a* and *b*) [10].

As shown in Fig. 1, an optical fiber of a length L is considered and an arbitrary strain distribution $\epsilon_m(x)$ is experienced only between the abscissas noted a and b. Note that no assumption is imposed on the shape of $\epsilon_m(x)$ excepted that it is assumed to be null if $0 \leq x < a$ and $b < x \leq L$. These two parts between the abscissas $x = 0$ and $x = a$ and between $x = b$ and $x = L$ are used to connect an optical interrogator and to make an optical termination.
In addition, the strain lag parameter β is assumed to change along the optical fiber as shown in Fig. 1:

$$\beta = \begin{cases} \beta_1 & 0 \leq x < a \\ \beta_2 & a \leq x \leq b \\ \beta_1 & b < x \leq L \end{cases} \qquad (2)$$

This leads to write the boundaries and continuity conditions and consequently the solution $\epsilon_f(x)$ as the following:

$$\begin{cases} \epsilon_{f1}(L) = 0 \text{ and } \epsilon_{f3}(L) = 0 \\ \left.\frac{d\epsilon_{f1}(x)}{dx}\right|_{x=a} = \left.\frac{d\epsilon_{f2}(x)}{dx}\right|_{x=a} \\ \left.\frac{d\epsilon_{f2}(x)}{dx}\right|_{x=b} = \left.\frac{d\epsilon_{f3}(x)}{dx}\right|_{x=b} \end{cases} \qquad \epsilon_f(x) = \begin{cases} \epsilon_{f1}(x) & 0 \leq \mathrm{x} < a \\ \epsilon_{f2}(x) & a \leq \mathrm{x} \leq b \\ \epsilon_{f3}(x) & b < \mathrm{x} \leq L \end{cases} \qquad (3)$$

A general solution $\epsilon_f(x)$ for any arbitrary $\epsilon_m(x)$ can be obtained from Eq. 1 to 3. The reader can find more details in [10].

3. Experiment and results

The results of an experiment are now presented to point out the impact of the strain-lag parameter values on the strain profiles measured $\epsilon_f(x)$ in comparison with the strain profile $\epsilon_m(x)$ and also to validate the general solution proposed. The experiment consisted in making a tensile test on a specimen made of two plates, in steel and aluminum, bonded together (with an epoxy adhesive) as shown in Fig. 2. This specimen was instrumented on both sides by two monomode optical fibers with different coatings: polyimide (external diameter: 145 µm) and acrylate (external diameter: 250 µm).

The two optical fibers were attached on the specimen with a two-component epoxy adhesive (Araldite 2014-2) over three different lengths (20 cm, 10 cm and 5 cm). A uniaxial tensile was performed on the specimen (dimensions: 80 cm × 5 cm × 5 mm) to create two uniform strain fields in each plates of the assembly given that the Young modulus for steel and aluminum plates are respectively equal to 200 GPa and 69 GPa. A servohydraulic testing system applied a constant tensile force of 5 kN on the specimen during the strain profiles measurements obtained with a high spatial resolution distributed optical fiber interrogator (0.65 mm gage pitch, 1.3 mm gage length, model: Luna ODISI-B).

(a) (b)

Fig. 2. Description of the experiment. (a) Photography of the instrumented specimen under tensile test. (b) Schematic presentation of the specimen instrumentation.

Fig. 3 presents the strain profiles of the polyimide and acrylate coated optical fibers for the three bonding lengths (violet curves). It can be observed that the strain profiles measured with the polyimide-coated optical fiber is composed of two clearly visible constant strain distributions, as expected, around 100µm/m and 300µm/m in the steel and aluminum plates, respectively. Note also that the level of noise (due in large part to vibrations of the hydraulic testing system) increases over the length of the optical fiber. Despite this, the maximum strain values are almost the same for three bonding lengths of polyimide-coated optical fiber. On the other hand, the acrylate-coated optical fiber gives different measurements. Firstly, the two constant strain distributions are not distinguishable and secondly, the maximum strain values in the steel and aluminum plates decreases with the bonding lengths. These phenomena are due to the strain transfer of the optical fiber which depends on the type, the number of the optical fiber coatings as well as the interface strength between themselves and with the substrate. From the measurements, it can be observed that the polyimide-coated fiber has a shorter strain transfer length than the one with an acrylate coating. For this reason, polyimide coated fiber is recommended for high resolution distributed strain measurements.

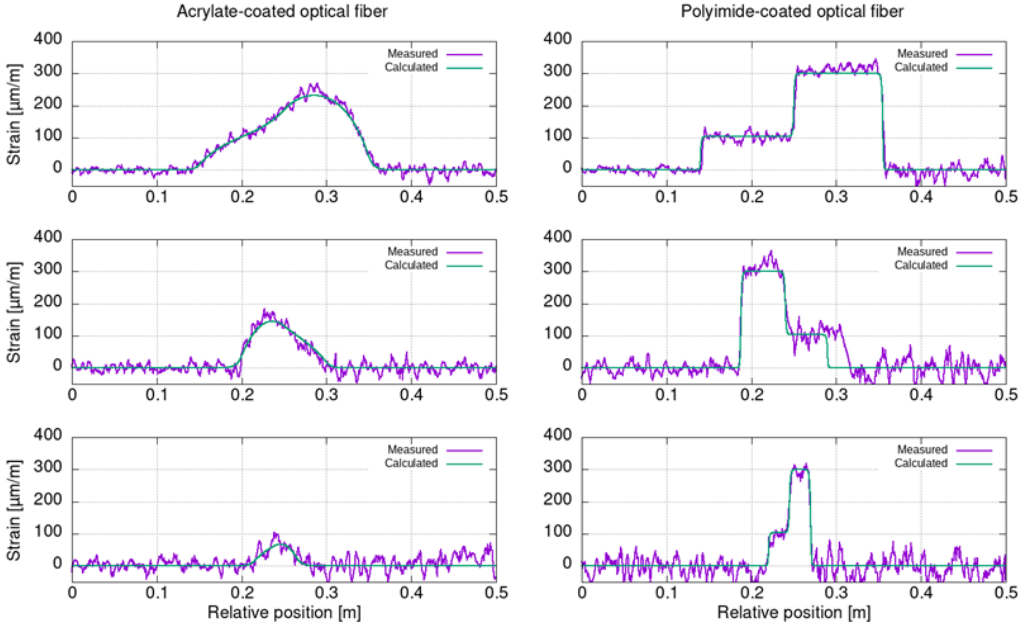

Fig. 3. Comparison of the strain profiles measured and calculated from the general solution: (a) for the sample instrumented by acrylate-coated optical fiber, (b) for the sample instrumented by polyimide-coated optical fiber.

These results highlight the importance of considering the optical fiber's strain transfer effect for a correct interpretation of measurements, especially in the case of strain gradients. The modeling presented at the beginning of the paper has been shown that the strain lag parameters β_1 and β_2 drive the strain transfer mechanism. In [10], a method for estimating them is proposed and some values have already been obtained for the same optical fibers and with an identical procedure of installation and with the same adhesive as the one used in the experiment presented in this paper. These values are given in Table 1 and they are used to calculate the strain profiles $\epsilon_f(x)$ from the general solution proposed in [10].

Acrylate-coated optical fiber		**Polyimide-coated optical fiber**	
β_1 [m^{-1}]	β_2 [m^{-1}]	β_1 [m^{-1}]	β_2 [m^{-1}]
180	31	1500	1050

Table 1. Strain lag parameters

The results of the strain profile's calculations are also plotted in Fig. 3 (green curves) for a comparison with the measured strain profiles (violet curves). A very good agreement between the measured and calculated strain profiles can be noticed. The discrepancy visible for the polyimide-coated optical fiber bonded in steel plate over a bonding length of 10 cm is due to too much unwanted bonding length (2cm). The results show thus the validity of the general solution proposed in this paper. The method can be applied for any arbitrary strain profile $\epsilon_m(x)$. Note also that it requires low computation time.

Conclusion

In this paper, the importance of optical fiber's strain transfer effect is highlighted for high resolution distributed strain measurements. To describe this phenomenon, an analytical modeling is used to derive a general solution of a governing equation which shows that some key parameters, called strain lag parameters, drive the strain transfer mechanism.

It is worth underlying that the strain transfer phenomenon depends both on the type of optical fibers (or cables) used as a sensor and on its attachment to the surface or embedding in the material. The strain lag parameters defined in the general solution permits the completely characterization of this phenomenon. However, the estimations of these parameters from the geometrical and mechanical properties of the optical fiber sensors and the attachment conditions may often be inaccurate due to the fact that some parameters, such as interface stiffness parameters, are hardly known and difficult to measure. It is then recommended to determine experimentally the strain lag parameters. For this, the methodology proposed in [10] can be used.

References

1. Bado, M.; Casas, J. 2021. "A review of recent distributed optical fiber sensors applications for civil engineering structural health monitoring". *J. Sens*., 21(15):1818.
2. Glisic, B. 2013. "Distributed fiber optic sensing technologies and applications—An overview". *ACI Spec. Publ*. 292:118.
3. Ansari, F.; Libo, Y. 1998. "Mechanics of Bond and Interface Shear Transfer in Optical Fiber Sensors". *J. Eng. Mech*. 124:385-394.
4. Henault, J.-M. 2013. "Approche Méthodologique pour l'Evaluation des Performances et de Ladurabilité des Systèmes de Mesure Répartie de Déformation: Application à un Câble à Fibre Optique Noyé dans le Béton". *Ph.D. Thesis*, Université Paris-Est, Paris, France.
5. Alj, I.; Quiertant, M.; Khadour, A.; Grando, Q.; Terrade, B.; Renaud, J.-C.; Benzarti, K. 2020. "Experimental and numerical investigation on the strain response of distributed optical fiber sensors bonded to concrete: Influence of the adhesive stiffness on crack monitoring performance". *J. Sens*. 20(18):5144.
6. Li, D.; Li, H.; Ren, L.; Song, G. 2006. "Strain transferring analysis of fiber Bragg grating sensors". *Opt. Eng*. 45(2):024402.
7. Tan, X.; Bao, Y.; Zhang, Q.; Nassif, H.; Chen, G. 2021. "Strain transfer effect in distributed fiber optic sensors under an arbitrary field". *Automat. Constr*. 124:103597.
8. Wang, H.; Xiang, P. 2016. "Strain transfer analysis of optical fiber-based sensors embedded in an asphalt pavement structure". *Meas. Sci. Technol*. 27:075106.
9. Bassil, A.; Chapeleau, X.; Leduc, D.; Abraham, O. 2020. "Concrete crack monitoring using a novel strain transfer model for fiber optics sensors: An imperfect bonding theory". *J. Sens*. 20(8):2220.
10. Chapeleau, X, Bassil, A. 2021. "A General Solution to Determine Strain Profile in the Core of Distributed Fiber Optic Sensors under Any Arbitrary Strain Fields". 21(16): 5423.